Tau_b: A Metabolic Neuroimaging Biomarker

William D. Rooney[1], Xin Li[1], John W. Grinstead[2], Edward A. Neuwelt[3], and Charles S. Springer, Jr. [1]

[1]*Advanced Imaging Research Center, Oregon Health & Science University, Portland, Oregon, United States,* [2]*Siemens Healthcare, Portland, Oregon, United States,* [3]*Blood-Brain-Barrier Program, Oregon Health & Science University, Portland, Oregon, United States*

Introduction: Capillary lumen water is "well-mixed" (1). During passage through a typical ^1H_2O MRI voxel [(1 mm)^3], H_2O molecules exchange into and out of blood cells, and collide with the capillary wall, many times. The escape probability [equilibrium extravasation] is the inverse of the mean H_2O molecule lifetime in a blood capillary (τ_b). $\tau_b = 0.5 \cdot r \cdot (P_W')^{-1}$; with r and P_W' the voxel *mean* capillary radius and water permeability coefficient, respectively (2). With sufficient compartmentalized paramagnetic contrast agent concentration, [CA], the ^1H_2O inversion recovery (IR) is non-mono-exponential and compartmental H_2O lifetime (τ) values can be determined (2,3). But it is likely impossible to reach the required blood [CA] *in vivo* (4). However, even with mono-exponential IR, if [CA] is *varied*, τ values can be measured (2,4). Originally, blood [CA] was deliberately varied (animal model) to obtain τ_b (5). Then it was shown that, in the human brain, a single CA bolus, (Dynamic-Contrast-Enhanced) DCE-MRI, is sufficient because [CA] increases and decreases during the bolus passage: CA does not extravasate in the normal brain (6). But the approved monomeric Gd(III) chelate CAs do extravasate in brain tumors. Here, we use a superparamagnetic iron oxide (SPIO) nanoparticle CA that can be bolus injected (7). During the first pass, and indeed the first hour, it does not extravasate even from tumor capillaries. We use the 2-site-exchange (2SX) shutter-speed paradigm (SSP) DCE-MRI analysis (6).

Methods: DCE-MRI quantitative T_1 (qT_1) data were acquired on a Siemens 3T Tim Trio instrument with a multislice 2D GRE-EPI based sequence with a (128)^2 image matrix, resulting in nominal (2 mm)^3 isotropic resolution (8). Points were obtained in the CA steady-state before, and after IV injections of Ferumoxytol [Fe-tol; MW = 750 kDa] (7), fractionated into 3 doses [1:2:4] totaling 4 mg(Fe)/kg. The qT_1 acquisitions were initiated 120 s after each Fe-tol injection, during the plasma CA steady-state period; *i.e.*, when plasma [CA] was uniform and constant: [CA] was larger after each successive injection. This was a multi-day study, and a similar protocol using the momomeric GdHPDO3A CA, was conducted 24 hr prior to the Fe-tol MRI session. Six *glioblastoma multiforme* [GBM] subjects consented. Data are also reported from a separate 7T study of 2M/4F healthy controls using GdHPDO3A.

Results: **Fig. 1** displays sample data from a 52 y M GBM subject. In the center is an axial qT_1-w image obtained 30 min after GdHPDO3A injection. The CA-enhancing tumor is clearly visible at the lower left. Inset are data (crosses) obtained from 4 representative ROIs [frontal WM, thalamus, putamen, and tumor; ellipses] during Fe-tol injections of this subject. Each plot shows the R_{1b}-dependence of R_{1t}. [$R_1 \equiv T_1^{-1}$: R_{1b} is taken at 4 times from a sagittal sinus ROI, each R_{1t} at the same 4 respective times from the ROI indicated]. If the tracer pharmacokinetic paradigm [$\tau_b \rightarrow 0$] obtained, the R_{1t},R_{1b} plot would be linear. None are, and all are well fitted by 2SX SSP expression (4,6) curves with τ_b, v_b, and R_{1exv} varied [v_b is the blood volume fraction, R_{1exv} the pre-exchange extravascular ^1H_2O R_1]. The population- and ROI-averaged v_b and τ_b values are given in the **Table** [NA, normal-appearing]. For comparison, the normal WM and GM healthy control biomarkers are also listed. In the GBM brain, the v_b values are generally smaller than normal, except in the tumor. The τ_b values in the NA-GBM brain are rather normal, and most definitely non-zero. However, in tumor tissue τ_b is increased by an order-of-magnitude. Is this remarkable increase because r is increased, P_W' is decreased, or both? In separate analyses, we have found - for cells in suspension, and in breast tumors and in myocardium *in vivo* - the mean intracellular water molecule lifetime (τ_i) is dominated by the cytolemmal P_W coefficient and not the cell radius. Furthermore, P_W has passive and active components (3). Three facts point to a dominant P_W'(active) component in the MS brain, where τ_b is also increased: 1.) ^{31}PMRSI shows PCr and ATP are reduced [~15%] in MS-NAGM (unpub.), 2.) ^{23}NaMRSI shows tissue Na content [likely Na_i] is increased [~28%] in MS brain (9), and 3.) τ_b is significantly increased [almost doubled] in MS lesions (unpub.). It is well-known that MS lesion capillaries are CA-permeable, and those in GBM tumor tissue even more so (7). There is little doubt this is due to widened para(endothelial)cellular pores. Thus, paracellular water extravasation [a P_W'(passive) pathway] must also increase. But this would make τ_b *decrease*. The conclusion is inescapable that the large τ_b increase observed must be dominated by a large P_W'(active) decrease in the GBM tumor.

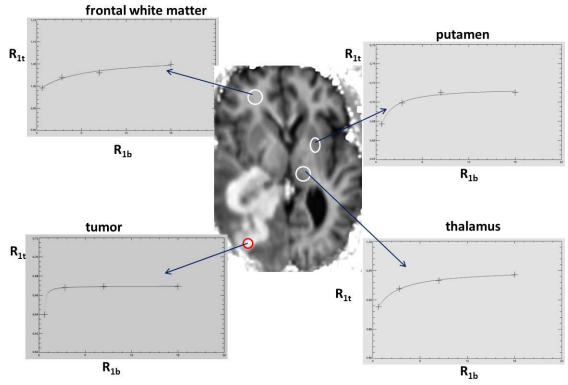

Table 1 Human Brain	ROI SSP Values	
	v_b	τ_b (s)
Healthy Controls (n = 6)[a]		
NWM	0.014	0.345
NGM	0.031	0.403
Glioblastoma (n = 6)[b]		
NA-frontal WM	0.008	0.44
NA-thalamus	0.017	0.38
NA-putamen	0.012	0.43
tumor	0.046	5.55

Discussion: The mean intracellular water molecule lifetime [τ_i] is dominated by active trans-membrane water cycling [10^{12} H_2O molecules/s/cell] (3). This process accompanies the active trans-membrane osmolyte cycling paced by the driving cell membrane ATPase transporter. For mammalian cells, this is the Na^+/K^+ATPase [NKA] pump, possibly the most important enzyme in biology. The τ_i magnitude is sensitive to the ATP_i and K_o^+ substrates of, and to specific inhibitors of, the driving ATPase transporters (3,10,11). **Fig. 2** is a cartoon of the "gliovascular unit" (12). Endothelial [gray], neuroglial [pink], and neuronal [blue] cells, in proximity with synaptic dimensions, act in exquisite metabolic synchrony (12,13). Active trans-membrane water cycling processes are indicated with stars. A cascade of these could constitute the P_W'(active) pathway [2d]. Possible P_W'(passive) pathways, simple transcellular H_2O diffusion across cell membranes [2b], transcellular transport through membrane aquaporin H_2O channels and/or transcellular leakage through membrane transporters [2c] are also shown. The paracellular H_2O pathway is shown as [2a], but this caries a miniscule flux compared with transcellular pathways. Our results strongly suggest that the P_W'(active) pathway [2d] dominates the τ_b magnitude. If this changes in parallel with changes in "Magistretti Metabolic Mechanism" [2e,f,g] fluxes (12,13), τ_b provides a high-resolution MRI biomarker sensitive to changes in cerebral neuronal activity. The lower the NKA activity, the larger the τ_b value. If this is true, cells in the GBM tumor have extremely slow NKA activity.

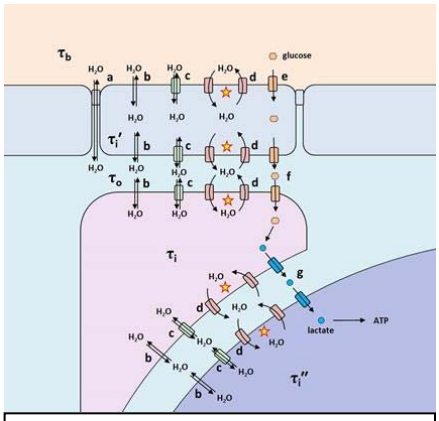

Figure 2. Gliovascular unit water exchange mechanisms determining mean water molecule lifetimes in blood (τ_b, beige), interstitium (τ_o, aqua), and endothelial (τ_i', gray), neuroglial (τ_i, pink), and neuronal (τ_i'', blue) cell spaces. The equilibrium paracellular (a), simple diffusion (b), facilitated transcellular (c), and active water cycling (d, stars) pathways are indicated, as are "Magistretti steps" (e,f,g).

Grant Support: NIH: RO1-NS040801; UO1-CA154602; R44 CA180425.

References: **1.** Strijkers, *et al*, *MRM* **61:**1049-1058 (2009). **2.** Labadie, *et al*, *JMR B* **105:**99-112 (1994). **3.** Zhang, *et al*, *Biophys J* **101**:2833-2842 (2011). **4.** Landis, *et al*, *MRM* **42:**467-478 (1999). **5.** Schwarzbauer, *et al*, *MRM* **37:**769-777 (1997). **6.** Rooney, *et al*, *PISMRM* **11:**2188 (2003). **7.** Gahramanov, *et al*, *Int J Radiat Oncol Biol Phys* **79:**514-523(2011). **8.** Grinstead, Rooney, *PISMRM* **16:**3084 (2008). **9.** Inglese, *et al*, *Brain* **133:**847-857 (2010). **10.** Poirier-Quinot, *et al*, *PISMRM* **14:**1176 (2006). **11.** Zhang, Balschi, *PISMRM* **21:**4045 (2013). **12.** Abbot, *et al*, *Nat Rev Neurosci* **7:**41-53 (2006). **13.** Lee, *et al*, *Nat* **487:**443-448 (2012).